

# Analysis of precipitating clouds using precipitable water vapour

\*Archana S, Shanmugha Sundaram G A, Soman K P

Center for Excellence in Computational Engineering and Networking, Amrita Vishwavidyapeetham University, Amritanagar, Coimbatore-641112, T.N., India.

\*Corresponding author: E-Mail: sarchana91@gmail.com

## ABSTRACT

The detection of precipitating clouds is necessary for weather prediction and climate researches. Precipitation occurs by condensation when the atmosphere is saturated with water vapour. The aim of the study is to discuss about the variations of Precipitable Water Vapour (PWV) in the case of such clouds. The brightness temperature data of  $6.7\mu\text{m}$  water vapour channel is primarily used in this study. The saturation mixing ratio can be calculated using temperature and pressure profile data. The study on PWV enhances the weather forecasting models and meteorological studies. In this study, the PWV for different precipitating clouds are estimated for a period of January-December 2014.

**KEY WORDS:** Precipitable water vapour, Upper tropospheric humidity, Brightness temperature, Precipitating clouds.

## 1. INTRODUCTION

Classification of clouds plays a major role in forecasting the weather phenomena. Clouds can be classified into low-level, mid-level and high-level clouds. The detection of rainy clouds plays a crucial role in weather forecasting. A reliable automated system to provide cloud datasets is necessary for climatic studies. But the variability in cloud forms, viewing angles, atmospheric conditions etc. made it a complex and difficult task. Clouds largely reduce diurnal range of surface air temperature by decreasing the solar radiation.

Clouds can be distinguished based on certain parameters such as brightness temperature, height, pressure and so on. Another important parameter is Precipitable Water Vapour (PWV). Precipitable Water Vapour is the depth of water in the atmospheric column, when all the water in that column is condensed and precipitated. The standard techniques to measure PWV include Radiosondes, LASER and LIDAR systems, ground-based microwave radiometers etc.

The precipitable clouds can be classified into Nimbostratus, Stratocumulus, Altostratus, Cumulonimbus, Stratus, Cumulus etc. Nimbostratus are thick, dark clouds which produces high intensity of rain. Altostratus are middle-level clouds which produces light precipitation and when the precipitation increases altostratus clouds get thicken into Nimbostratus clouds. Cumulonimbus clouds are vertically growing clouds associated with thunderstorms or showers. Stratocumulus clouds are low-level clouds which produces light rain or snow. Stratus clouds are low-level, uniform, featureless clouds. Occasionally stratus clouds become dark, but produce little precipitation, which makes it possible to distinguish from Nimbostratus clouds. Cumulus clouds are cotton-like clouds which produces showers.

The cloud cover and water vapour can be measured from ground observations and satellite observations. But, the meteorological satellites provide better observations for a wide view of angle compared to ground observations. Clouds have strong correlation with surface temperature. They alter the earth's radiation process by cooling and warming earth surface. Therefore, the need for study about clouds becomes necessary.

The PWV is an important parameter to study the Energy Budget but, is difficult to measure. The Precipitable water shows seasonal and annual variations due to changes in moisture content in maritime and continental air masses. The PWV values for each cloud will differ from each other. In this paper, the variation of PWV for clouds such as Nimbostratus, Altostratus and Stratocumulus clouds are studied.

The PWV gives an idea about the precipitation produced by each cloud. Precipitation can affect navigation. The shift in summer precipitation due to greenhouse effect produces more rainy days which in turn causes more aircraft accidents. Shen and Smith, formulated a multi-parameter model for estimating precipitable water beyond certain pressure levels using the satellite infrared spectrometer B radiance data.

The remaining of the paper is organized as follows. Section II describes the different datasets used for the study. Section III presents the methodology used and Section IV explains the results and analysis. Finally, Section V concludes the paper.

**Datasets:** Different sets of data are involved in the study of PWV. The detailed descriptions of data are given below:

**Gridsat Data:** The GRIDSAT data from NOAA's National Climatic Data Centre is used for the study. GRIDSAT data provides observations from infrared window, infrared water vapor and visible channels for each 3hr time slots, are widely used for climatic researches. Brightness temperature data of geostationary satellites are obtained from GRIDSAT dataset in NetCDF format. In this study, brightness temperature data from infrared water vapour channel  $6.7\mu\text{m}$  is used for the analysis. The GRIDSAT data are inter calibrated using calibration data of International Satellite Cloud Climatology Project (ISCCP). GRIDSAT data are gridded ISCCP B1 data with a resolution of 8 km.

GRIDSAT data is a collective of data obtained from the satellites such as GOES 13, GOES 15, FY 2-E, Meteosat 7, Meteosat 10 etc.

**GFS MODEL:** Global Forecast System (GFS) is a weather prediction model created by National Centers for Environmental Prediction (NCEP), and it runs 4 times per day to produce forecast 16 days in advance. GFS model provides observations from temperature, humidity, wind, precipitation etc. The data for January-December 2014 is used for the study. The resolution of GFS data is  $0.5^\circ \times 0.5^\circ$ . The data of GFS model are obtained as .grib format. The temperature height profiles can be obtained from GFS data for each locations.

**Student's cloud observation on-line (s'cool) project:** S'COOL is a project by National Aeronautics and Space Administration Langley Research Centre for students interested in cloud related studies. The detailed study of different clouds is done in this project. NASA Langley Atmospheric Science Data Centre stores the information submitted by students and the data from other atmospheric science research projects. From the satellite data, the cloud properties, altitude, temperature etc. will be detected using certain algorithms and is compared with the stored data, so as to provide an archive of reliable cloud data. The satellite observations are obtained from the CERES (Clouds and the Earth's Radiant Energy System) sensor of NASA's Terra satellite. The Terra satellite was launched on 18<sup>th</sup> December, 1999 and it has five sensors- ASTER, CERES, MODIS, MISR and MOPITT. CERES has three channels- short wave (0.3-5  $\mu\text{m}$ ), long wave (0.3-100  $\mu\text{m}$ ) and window (8-12  $\mu\text{m}$ ). It provides a spatial resolution of 20 km at nadir. The CERES instrument consists of two scanning radiometers: FM-1 and FM-2.

## 2. METHODOLOGY

NOAA operates on GOES systems which contains multiple satellites for continuously observing the earth. The GOES variable (GVAR) is the retransmission format for the processed meteorological data measured by Sounder and Imager instruments. The GVAR comprises of 12 blocks from 0 to 11 and the blocks 0 to 10 are send contiguously and the block 10 is followed by variable block 11, according to the nature of data available for transmission. The number of words in the Information Fields of GVAR Blocks 0-10, for a single scan can be computed as  $8,280 + 39 \times N$  where N is the number of mirror 4-pixel groups, and it ranges from 8,280 to 212,484 words. Block 11 contains non-imager data while blocks 0-10 contain imager data. The lower limit for GVAR block is 32,208 bits which include 10,032 bits synchronization code block, 720 bits header, 16 bits CRC block and 21,440 bits information field. The bandwidth can be calculated from the blocks. The required bandwidth for non-scan related data, is constant time-dependent and for scan-associated data, bandwidth is dependent on scanning width of instrument. The GVAR data is transmitted from the spacecraft at a carrier rate of 2,111,360 bps. The transmission delays occur before the user receives the data. Finally encoding takes place in three stages. Due to bandwidth limitations the Imager does not contain the earth location array, but the Sounder is provided with data which maps each pixel to earth lat/lon point. GVAR contains both calibration coefficients and scaling coefficients. Users can get the radiance from the raw data using these calibrations.

For imager channels of geostationary satellites the raw data stream of radiance counts are 10 bits long. The radiance values are then calculated from raw data by:

$$R = \frac{x-b}{m} \quad (1)$$

Where the radiance in  $\text{mW}/(\text{m}^2 \cdot \text{sr} \cdot \text{cm}^{-1})$  is denoted as R and the count values as x. b is the scaling bias and m is the scaling gain. The brightness temperature is then obtained by

$$T_{\text{eff}} = \frac{c_2 \cdot n_u}{\ln(1 + \frac{c_1 \cdot n_u^3}{R})} \quad (2)$$

Where  $T_{\text{eff}}$  is the effective temperature and  $n_u$  ( $\text{cm}^{-1}$ ) is the central wave number of the channel. The two radiation constants are given as  $c_1 = 1.191066 \times 10^{-5}$  ( $\text{mW} \cdot \text{m}^2 \cdot \text{sr}^{-1} \cdot \text{cm}^4$ ) and  $c_2 = 1.438833$  ( $\text{cm} \cdot \text{K}$ ). The actual temperature can be obtained from the effective temperature.

$$T = a + b * T_{\text{eff}} \quad (3)$$

Where a and b are bias and gain coefficients which depend on observation channels.

The  $6.7\mu\text{m}$  channel gives information about moisture content in upper troposphere. The brightness temperature data from  $6.7\mu\text{m}$  channel is used for Upper Tropospheric Humidity (UTH) calculation. Soden and Bretherton derived an analytical expression for relative humidity and brightness temperature from  $6.7\mu\text{m}$  channel. UTH is defined as the measure of relative humidity of a level varying from 600mb to 300mb.

$$UTH = \frac{\exp(a+b \cdot T_b) \cos(\theta)}{P_0} \quad (4)$$

Where  $\theta$  is the satellite viewing zenith angle, a and b are least square fit slope and intercept of the regression line as defined by the empirical relationship and  $P_0$  is the normalized pressure.  $T_b$  is the brightness temperature value.

The values  $a=31.5$  and  $b=-0.115\text{K}^{-1}$  obtained by Sorden and Bretherton in their study are used here. These coefficients are calculated by comparing the brightness temperature of water vapour channel with the upper tropospheric humidity values of same temperature and pressure profiles. According to Sorden and Bretherton, these values are consistent with theoretically expected values and these values are expected to have little seasonal

variations. The advanced study of UTH can help in the study of sensitivity if earth's climate towards greenhouse gases.

The expression for normalized pressure is given by

$$P_0 = \frac{p(T=240K)}{P_1} \quad (5)$$

Where  $p_1=300\text{hPa}$  and  $p(T=240\text{K})$  is the pressure at the level where the temperature is 240K. The water vapour mixing ratio can be defined as the ratio of mass of water vapour to mass of dry air (in g/kg) and is denoted as  $q_v$ .

$$q_v = q_s * UTH \quad (6)$$

Where  $q_s$  is the saturation mixing ratio. Saturation mixing ratio is the maximum amount of water vapour that the air can hold for a particular temperature and pressure and can be calculated as follows:

$$q_s = \frac{0.622 * e}{P - e} \quad (7)$$

Where  $q_s$  is the saturation mixing ratio at pressure  $P$  and  $e$  is the vapour pressure. The expression for saturation vapour pressure can be given as,

$$e = 6.11 * \exp\left(\frac{17.27 * t}{273.3 + t}\right) \quad (8)$$

Where  $e$  is the vapour pressure in hPa and  $t$  is temperature in  $^{\circ}\text{C}$ . Using the above parameters, PWV can be calculated as,

$$PWV = \frac{1}{g} \int q_v dp \quad (9)$$

Where the incremental change in pressure is denoted as  $dp$  and PWV is the Precipitable water vapour in  $\text{kg}/\text{m}^2$  or mm of water.

### 3. RESULTS AND ANALYSIS

The PWV values for the clouds Nimbostratus, Altostratus and Stratocumulus are plotted. The PWV values of the clouds for a period of January- December 2014 are calculated. Fig.1. shows the brightness temperature of a region obtained from the  $6.7\mu\text{m}$  water vapour channel. The different range of brightness temperature is indicated by false colours. The lower values of brightness temperature are indicated by dark blue and the higher values are indicated by red as per the colour scale in Fig.1.

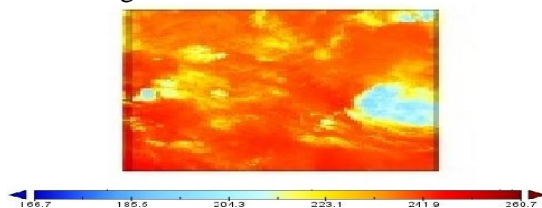


**Fig.1. Brightness temperature obtained from  $6.7 \mu\text{m}$  channel, in Kelvin**

Fig.2 shows the variation of PWV for different precipitating clouds. In Fig.2 the months are plotted in x-axis and PWV values are plotted in y-axis.

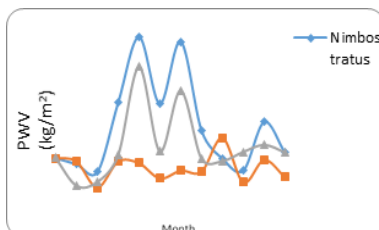


**Fig.2. PWV values of Nimbostratus, Altostratus and Stratocumulus clouds in  $\text{kg}/\text{m}^2$**

The clouds are showing linear variations for PWV in the graph. In Fig.2, it is observed that the Nimbostratus and Stratocumulus clouds are showing similar patterns for PWV values. Nimbostratus and Altostratus shows low PWV in March and October and, Nimbostratus and Stratocumulus clouds have a high peak for PWV in May and July. In September, Altostratus shows high value and in February and March, Stratocumulus hold low PWV values.

The highest PWV values shown by Nimbostratus clouds are  $45.345 \text{ kg}/\text{m}^2$  in May and  $44.0676 \text{ kg}/\text{m}^2$  in July. Nimbostratus clouds possess low PWV values  $8.2064 \text{ kg}/\text{m}^2$  and  $8.6429 \text{ kg}/\text{m}^2$  in March and October respectively. Altostratus shows highest PWV value  $17.6169$  in September and lowest value  $3.9688 \text{ kg}/\text{m}^2$  in March. Similarly, Stratocumulus clouds gives high PWV  $37.0855 \text{ kg}/\text{m}^2$  in May and low PWV  $4.482 \text{ kg}/\text{m}^2$  in February.

During the month May, the variation of PWV for Nimbostratus and Altostratus are quite noticeable as the PWV value for Nimbostratus is  $45.345 \text{ kg}/\text{m}^2$  and PWV for Altostratus is  $10.669 \text{ kg}/\text{m}^2$ . During the month March, Nimbostratus, Altostratus and Stratocumulus clouds possess lower values for PWV. After March, Nimbostratus and Stratocumulus clouds are increasing linearly and reach the peak in May.

From Fig.2, it is observed that the Nimbostratus is having high PWV values when compared to other clouds and Altostratus is having less variation for PWV values when compared to other clouds. Stratocumulus shows moderate variation for PWV as it produces less precipitation compared to nimbostratus and high precipitation compared to Altostratus clouds. The plot for Brightness temperature (K) of Stratocumulus, Altostratus and Nimbostratus clouds for a period of January-December 2014 is given in Fig.3.

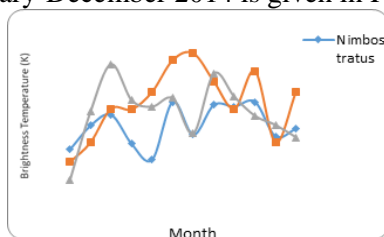


**Fig.3. Brightness temperature of Stratocumulus, Altostratus and Nimbostratus clouds in Kelvin**

In Fig.3, the Altostratus clouds and Stratocumulus clouds shows high brightness temperature values compared to Nimbostratus clouds. It is observed that the PWV values for the clouds increases with a fall in brightness temperature and also decreases with an increase in brightness temperature.

It is analyzed that the Nimbostratus, Altostratus and Stratocumulus clouds are showing a zigzag pattern for brightness temperature. Nimbostratus shows low PWV in May and high PWV value in June and October. It is observed that the brightness temperature of Stratocumulus clouds increase linearly from its lower value in January and reaches maximum value in March. The brightness temperature of Stratocumulus clouds linearly decreases after the month August. Altostratus clouds also hold a lower value in January and it reaches its peak in July.

Nimbostratus shows high brightness temperature 238.99 K in June and October and shows low brightness temperature 231.12 K in May. The brightness temperature for Altostratus during January is 230.7937 K, which is lowest and possesses a higher value 245.6 K in July. In January, Stratocumulus clouds hold a lower value for brightness temperature 228.333K and a higher value 244.1K in March.

During July, both Nimbostratus and Stratocumulus clouds gives lower values while Altostratus reaches its peak in July. Usually warm air holds more water vapour than dry air. But, here it is observed that the PWV for Altostratus is 8.6081 kg/m<sup>2</sup>, which is very less when compared to other clouds and hence during July the precipitation produced by Altostratus clouds is very less compared to Nimbostratus and Stratocumulus clouds. During December, except Stratocumulus, both Nimbostratus and Altostratus clouds shows a slight increase in brightness temperature. It is observed that sometimes, even in the presence of precipitation clouds the rainfall may not take place. These rare scenarios are analyzed using the parameters Precipitable Water Vapour and Brightness Temperature.

Table.1.shows the calculated PWV values for Nimbostratus, Stratocumulus and Altostratus clouds during precipitation and when there is no precipitation.

**Table.1. PWV Values of Nimbostratus, Stratocumulus and Altostratus Clouds during Precipitation and without Precipitation in kg/m<sup>2</sup>**

Month	Nimbostratus		Stratocumulus		Altostratus	
	Precipitation	No Precipitation	Precipitation	No Precipitation	Precipitation	No Precipitation
January	51.0604	1.4952	13.1526	-	19.4811	2.2112
February	27.8096	1.1143	-	3.6019	57.9751	0.5582
March	19.3432	1.3667	5.4936	-	-	2.1599
April	37.9674	2.6522	5.0098	1.8420	22.7181	2.5534
May	19.2519	2.4218	-	2.5812	-	2.0923
June	25.3076	1.3225	14.4022	2.2035	-	2.2726
July	32.9290	2.2084	-	3.0917	-	8.6082
August	53.6438	2.4622	-	2.9408	-	5.2941
September	19.7749	-	-	1.1449	-	1.8415
October	28.5124	2.0217	20.8760	1.8998	-	1.8429
November	22.1209	-	8.0451	1.0076	23.4665	3.7037
December	26.9670	2.6346	-	1.0696	10.3325	3.3089

The change in PWV values during the different scenarios- precipitation and no precipitation are studied for the different precipitating clouds. It is observed from Table I, that the PWV values during precipitation are higher than PWV values during no precipitation. In Table I and Table II, spaces are left as some data are unavailable.

Nimbostratus clouds show a high PWV values 51.0604 kg/m<sup>2</sup> in January and 53.6438 kg/m<sup>2</sup> in August during the case of precipitation. It is observed that during precipitation, the Nimbostratus clouds shows low PWV values 19.3432 kg/m<sup>2</sup>, 19.2519 kg/m<sup>2</sup>, 19.7749 kg/m<sup>2</sup> in March, May and September respectively. Nimbostratus clouds are

low level clouds and are associated with continuous precipitation. As the PWV values increases the rate of precipitation also increases. In some exceptional cases, there will be no precipitation even in the presence of precipitating clouds. In such cases i.e., during no precipitation the PWV values are very low compared to the case when there is precipitation. From the available data, it is observed that Nimbostratus clouds show least PWV value  $1.1143 \text{ kg/m}^2$  in February and hence it does not produce precipitation.

Similarly, Stratocumulus clouds shows a PWV  $20.8760 \text{ kg/m}^2$  in October during precipitation, which is very less when compared to Nimbostratus clouds. The lowest value observed during precipitation for Stratocumulus clouds is  $5.0098 \text{ kg/m}^2$  in April. It is seen that, in the case of no precipitation, Stratocumulus clouds possess lower PWV  $1.0076 \text{ kg/m}^2$  during the month November, and higher PWV value  $3.6019 \text{ kg/m}^2$  in February, from the available data. In October, the PWV values obtained for Stratocumulus clouds, during precipitation and no precipitation are  $20.8760 \text{ kg/m}^2$  and  $1.8998 \text{ kg/m}^2$  respectively, shows a noticeable difference.

Altostratus clouds show a high PWV value  $57.9751 \text{ kg/m}^2$  and low PWV value  $0.5582 \text{ kg/m}^2$  in February. So it can be explained as, due to high PWV value altostratus produces precipitation in February and no precipitation occurs due to the drastic fall in the PWV value in the same month. From Table I it is seen that the difference between PWV values during precipitation and no precipitation cases are higher, in the same months. The sudden fall in the PWV values will affect the nature of precipitation.

The brightness temperature values for a period of January-December 2014 during precipitation and without precipitation are shown in Table.2. It is observed that, when the Brightness temperature is lower, the PWV values are higher and vice versa.

From Table.2, it is analyzed that the brightness temperature values of Nimbostratus, Stratocumulus and Altostratus clouds gives low values during precipitation when compared to that without precipitation.

In the case of precipitation, Nimbostratus exhibit higher brightness temperature value  $236.2 \text{ K}$  in June and lower brightness temperature  $217.7 \text{ K}$  in April. In the case of no precipitation, Nimbostratus shows a low brightness temperature  $238.1 \text{ K}$  in February and high value for brightness temperature  $247.1 \text{ K}$  in May. It is observed that Stratocumulus possess a high value of  $244.1 \text{ K}$  and a low value  $230.4 \text{ K}$ , during precipitation. In May, Stratocumulus exhibits a brightness temperature of  $249.5 \text{ K}$  and in November it exhibits  $236.9 \text{ K}$ , in the case of no precipitation. Altostratus holds a higher brightness temperature  $236.9 \text{ K}$  in December and a lower value  $218.6 \text{ K}$  in February, during precipitation. In the case of no precipitation, altostratus shows a high brightness temperature  $256.2 \text{ K}$  in October and a low brightness temperature  $232.3 \text{ K}$  in February. It is noticed that in February Nimbostratus, Stratocumulus and Altostratus clouds possess lower brightness temperature, in the case of no precipitation. In the scenario of no precipitation, both Stratocumulus and Altostratus clouds possess higher brightness temperature than the Nimbostratus clouds.

**Table.2. Brightness temperature values of nimbostratus, stratocumulus and altostratus clouds during precipitation and without precipitation, in kelvin**

Month	Nimbostratus		Stratocumulus		Altostratus	
	Precipitation	No precipitation	Precipitation	No precipitation	Precipitation	Non-precipitation
January	224	241	232.1	-	224.1	252.6
February	220.5	238.1	-	238	218.6	232.3
March	227.5	257.8	244.1	-	-	233.7
April	217.7	249.3	239	-	229.6	250.6
May	230.8	247.1	-	249.5	-	248.5
June	236.2	246.7	235.6	249.2	-	253.2
July	231.8	254.2	-	241.6	-	245.6
August	228.1	243.4	-	245.3	-	241.8
September	232.9	-	-	245.3	-	252.4
October	231.8	242.6	230.4	239.8	-	256.2
November	228.3	-	235.1	236.9	225.7	245.5
December	231.1	252.8	-	242.3	236.9	243.8

#### 4. CONCLUSION

The study of Precipitable Water Vapour variation for the Nimbostratus, Altostratus and Stratocumulus clouds are done. The water vapour absorbs radiations in sub-millimeter range and is more sensitive to greenhouse effect. The increasing interest in the study of water vapour has a vital role in the area of weather forecasting and climatic studies. The identification of precipitating clouds provides information about changes that occur in the atmosphere and facilitates the study on Energy budget. The change in climatic features results in the variation of cloud properties. The variation of PWV for precipitating clouds is studied. The analysis shows that the PWV values for Nimbostratus clouds are higher than Altostratus and Stratocumulus clouds. Currently, it becomes crucial to study the role of clouds

in climate changes for understanding the effects of global warming. The knowledge about precipitating clouds helps in aviation, marine navigation etc.

## 5. ACKNOWLEDGMENT

The GridSat data was provided by NOAA's National Climatic Data Center (NCDC) and GFS data was provided by NOAA National Operational Model Archive and Distribution System (NOMADS). I acknowledge Dr. K.P Soman, Head, Center for Excellence in Computational Engineering and Networking, Amrita Vishwa Vidyapeetham, for his valuable support and encouragement. Finally, I acknowledge the help rendered by Dr.P.Geetha, Center for Excellence in Computational Engineering and Networking, Amrita Vishwa Vidyapeetham.

## REFERENCES

- Changnon, Stanley A, Effects of summer precipitation on urban transportation, *Climatic Change*, 32 (4), 1996, 481-494.
- Dai, Aiguo, Kevin E Trenberth, and Thomas R Karl, Effects of clouds, soil moisture, precipitation, and water vapor on diurnal temperature range, *Journal of Climate*, 12 (8), 1999, 2451-2473.
- Erasmus D Andre, and Ruby van Rooyen, A Satellite Survey of Cloud Cover and Water Vapour in Morocco and Southern Spain and a Verification Using La Palma Ground-based Observations, Final Report. European Southern Observatory, 2006, 38.
- Erasmus D Andre, and Van Staden C.A, A satellite survey of cloud cover and water vapor in northern Chile, A study conducted for Cerro Tololo Inter-American Observatory and University of Tokyo, 2001.
- Erasmus D.A, Precipitable Water Vapour at SKA Telescope Candidate Sites: Derivation from raw in sonde data and a discussion of alternative measurement methods, Memorandum for the International Square Kilometre Array Telescope Project, 2005.
- Global Forecast System, Available: <https://www.ncdc.noaa.gov/data-access/model-data/model-datasets/global-forecast-system-gfs>.
- Kassomenos P.A, and Mc Gregor G.R, The interannual variability and trend of precipitable water over southern Greece, *Journal of Hydrometeorology*, 7 (2), 2006, 271-284.
- Knapp, Kenneth R, Globally gridded satellite (Grid Sat) observations for climate studies, 2012.
- Komajda, Raymond J, and Keith McKenzie, An introduction to the GOES IM imager and sounder instruments and the GVAR retransmission format, NASA STI/Recon Technical Report N 88, 1987.
- Maghrabi, Abdullrahman, and Al Dajani H.M, Estimation of precipitable water vapour using vapour pressure and air temperature in an arid region in central Saudi Arabia, *Journal of the Association of Arab Universities for Basic and Applied Sciences*, 14, 2013, 1-8.
- Marin, Julio C, Diana Pozo, and Michel Cure, Estimating and forecasting the precipitable water vapor from GOES satellite data at high altitude sites, *Astronomy & Astrophysics* 573, A 41, 2015.
- Shen, William C, and William L Smith, Statistical Estimation of Precipitable Water with Sirs-B Water Vapor Radiation Measurements, *Atmospheric Radiation*, 1, 1972.
- Smith, Stephen, and Ralf Toumi, Measuring cloud cover and brightness temperature with a ground-based thermal infrared camera, *Journal of Applied Meteorology and Climatology*, 47 (2), 2008, 683-693.
- Soden Brian J, and John R Lanzante, An assessment of satellite and radiosonde climatologies of upper-tropospheric water vapor, *Journal of Climate*, 9 (6), 1996, 1235-1250.
- Soden Brian J, and Rong Fu, A satellite analysis of deep convection, upper-tropospheric humidity, and the greenhouse effect, *Journal of climate*, 8 (10), 1995, 2333-2351.
- Soden, Brian J, and Francis P Bretherton, Interpretation of TOVS water vapor radiances in terms of layer-average relative humidities: Method and climatology for the upper, middle, and lower troposphere, *Journal of Geophysical Research, Atmospheres*, 101, 1996, 9333-9343.
- Students' Cloud Observations On-line, Available: <http://science-edu.larc.nasa.gov/SCOOL>.
- Terra Mission, eo Sharing Earth Observation Resources, Available: <https://directory.eoportal.org/web/eoportal/satellite-missions/t/terra>.
- Wahab M Abdel, and Sharif T.A, Estimation of precipitable water at different locations using surface dew-point, *Theoretical and applied climatology*, 51 (3), 1995, 153-157.
- Warren, Stephen G, Ryan M Eastman, and Carole J Hahn, A survey of changes in cloud cover and cloud types over land from surface observations, 1971-96, *Journal of Climate*, 20 (4), 2007, 717-738.